ADVANCED FUNCTIONAL MATERIALS
www.afm-journal.de

Virus-Tethered Magnetic Gold Microspheres with Biomimetic Architectures for Enhanced Immunoassays

Chang Su Jeon, Inseong Hwang, and Taek Dong Chung**

In immunoassays, non-specific bindings to biosensing surfaces can be effectively prevented by formation of biocompatible and hydrophilic self-assembled monolayer (SAM) on the surfaces. A thin gold (Au) layer on magnetic microspheres, 15 μm in diameter, enables facile SAM formation and thereby accepts second layer of filamentous virus scaffolds for the immobilization of functional proteins. The merger of the virus and SAM-Au protected microspheres not only provides exceptionlly dense antibody loading, but also resembles biological cellular structures that enhance ligand-receptor interactions. Site-specific biotinylation of filamenous viruses allows formation of free-standing virus threads (>1.0×10^{10}) on streptavidin-modified SAM-Au microspheres. The augmented yield of antibody loading, due to the increased surface to volume ratio, on virus-modified Au microspheres is confirmed by measuring fluorescence intensities. The bead-based immunoassays for the detection of cardiac marker proteins exhibit increased sensitivity of virus-Au microspheres, as low as 20 pg mL^{-1} of cardiac troponin I in serum, and extremely low non-specific adsorption when compared with bare polymer beads. This increased sensitivity due to filamentous morphology and SAM-Au layer demonstrates the feasibility of merging viruses with non-biological materials to yield biomimetic tools for the enhanced bead-based immunoassays.

1. Introduction

Recent outbreak of virus-based hybrid materials has enabled realization of highly selective and sensitive biosensors.[1] The benefits of the merger between virions and biosensing materials intuitively originate from the virion's capability of molecular recognition[2] and innate physical properties that stem from the phenotypic morphologies.[3] However, despite the functional advances in biosensors using virus hybrids, the detection systems largely remain in two-dimensional planar platforms, requiring relatively large sample volumes and greater time for analysis.[1]

In this paper, we demonstrate enhanced detection of protein biomarkers using Au-layered magnetic microspheres on which viral filaments are tethered in orientation-controlled manner. The magnetic Au microspheres, like many other typical microspheres, are compatible with flow cytometers, fluorescence-activated cell sorting (FACS) systems, and conventional fluorescence microscopes, requiring minute sample volumes, and allowing statistical analysis that raises credibility.[4] Importantly, in contrast to nanoparticles, the Au microspheres are eligible for the detection of small-molecule biomarkers in serum.

In biosensor development for immunoassays, preventing non-specific adsorption while providing high antibody loading is of primary importance. Since we had been experiencing a heavy non-specific binding to typical polymer beads when using blood or serum samples, we envisioned that covering the porous and sticky surfaces of the polymer beads with Au and thiol self-assembled monolayers (SAMs) should resolve the adsorption problem. The SAM molecules, if properly chosen, are able to prevent non-specific interactions between Au surface and analytes as well as to provide functional groups for protein conjugation.[5]

Filamentous bacteriophages, such as fd and M13, have nanostructured morphologies with contour length of ≈1 μm and diameter of ≈7 nm.[6] The viruses are comprised of five different kinds of structural proteins (pIII, pVI, pVII, pVIII, and pIX) that encase a single-stranded viral DNA. Among them, more than 2700 copies of the major coat protein pVIII serve for the assembly of filamentous structure with their ε-amino groups of Lys-8 and α-amino groups of N-termini being exposed, each of which have been successfully modified with macromolecules using chemical conjugation.[2c,7] A minor coat protein pIII, three to five copies per virion, has been dominantly used for the display of peptides and proteins (**Figure 1**).[8]

The filamentous morphology of the filamenous (fd) virus provides unique opportunity to construct bioinspired architectures because the virus has similar structural dimensions to many cellular threadlike structures that leverage various cellular functions. Furthermore, in biorecognition processes, such as ligand-receptor interactions, longer and flexible tethers and polyvalency have proved to be beneficial.[9] Indeed, in biological systems, neuronal cells are rich in neurites and filopodia that maximize the cellular interactions by forming synapses.[10] Leukocytes, macrophages, and some epithelial cells are covered with microvilli that facilitate cellular movement, adhesion,

C. S. Jeon, Dr. I. Hwang, Prof. T. D. Chung
Department of Chemistry
College of Natural Science
Seoul National University
Seoul 151-747, Korea
E-mail: inseong@snu.ac.kr; tdchung@snu.ac.kr

DOI: 10.1002/adfm.201202499

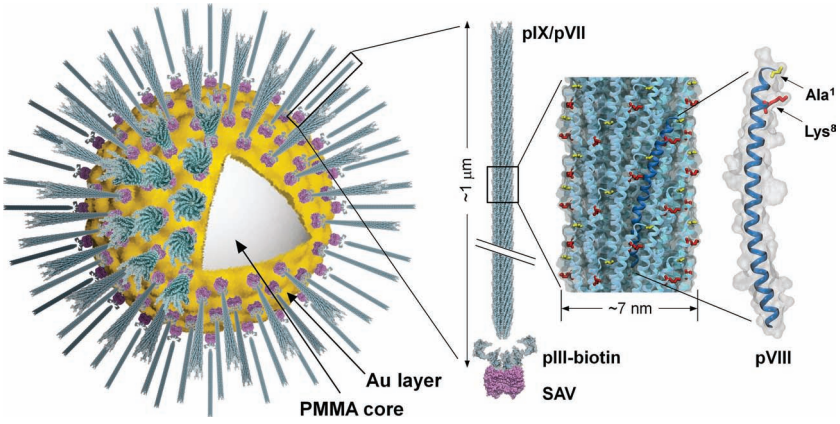

Figure 1. Schematic representation of the bioinspired virus-Au microsphere. A thin gold layer allows facile surface modifications by thiol SAMs followed by chemical conjugation of functional proteins, such as SAV (purple). The SAV-modified microspheres are decorated with pIII-biotinylated phage virions (pale blue) that have filamentous structure, resembling the surface morphology of some cells. The surface-exposed amine groups of N-terminal Ala-1 (yellow stick) and Lys-8 (red stick) of the viral major coat proteins (blue for a single pVIII unit) are used for the Staudinger ligation with primary antibodies to yield microspheres covered with high-density antibodies. Protein figures were generated using VMD[19] based on PDB code 1IFJ.

endocytosis, and exocytosis.[11] Similarly, some bacterial cells represent pili that help cell–cell interactions essential for mating; others have fimbriae that aid adhesion.[12] Based on these observations, we reasoned that the surface of Au microspheres, once modified with nanostructured filamentous virions, would have greater surface to volume ratio, mimicking biological architectures and thus allowing high degree of conjugation with functional molecules, such as antibodies. Such an increased ratio of antibody to biomarkers, together with three-dimensional Au-SAM protected surface of microspheres and microvilli-like long virus tethers, would provide improved performance compared to conventional 2D or 3D detection systems.

2. Results and Discussion

To keep the intact filamentous structure of the virions on microspheres, conjugation reactions should be devoid of intra- and intermolecular crosslinking of the virions, while not interfering with a directional binding of virion tips to microspheres. To that end, we selectively biotinylated pIII parts for the orientation-controlled immobilization of fd virions and thereby used the Staudinger ligation, a bioorthogonal and chemoselective crosslinking between azide and phosphine,[13] for the ligation of phage virions and antibodies (Figure S1 in the Supporting Information). Initially, we prepared SAM-protected Au beads using carboxyl-terminated hexa(ethylene glycol) undecane thiol, followed by streptavidin (SAV) conjugation using 1-ethyl-3-(3-dimethylaminopropyl)-1-carbodiimide hydrochloride (EDC) and *N*-hydroxysuccinimide (NHS). The Au-layered microspheres were stable in ethanol for 16 h, enough time for SAM formation. The bead system facilitated chemical conjugation of SAV on the SAM-modified Au microspheres using EDC-NHS in that the unreacted excessive EDC and NHS could be easily washed out. Next, we briefly evaluated the SAV conjugation using biocytin-Alexa Fluor 594. When the beads were pre-treated with free biotin, no fluorescence was observed after incubation with the fluorescent biocytin. By contrast, we observed strong fluorescence signals when the beads were directly incubated with the fluorescent biocytin (**Figure 2**a).

For the site-specific biotinylation of phage virions, a 14-mer bacterial biotin acceptor peptide (AP), GLNDIFEAQKIEWHE,[14]

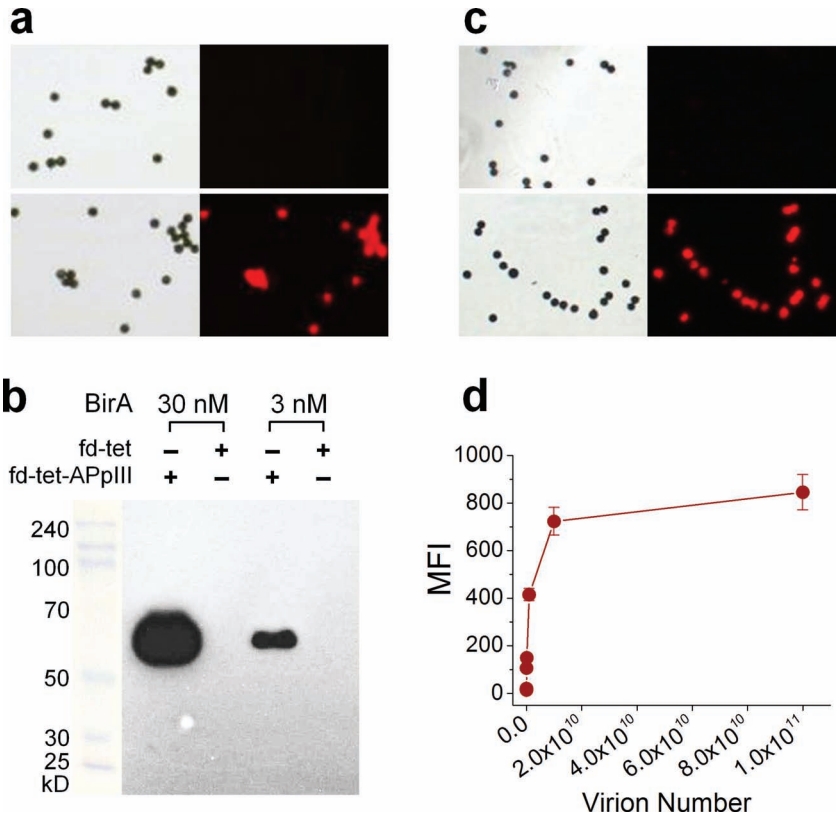

Figure 2. Optimization of surface modifications of Au microspheres with SAV and phage virions. a) The SAV-SAM on Au microspheres were pre-treated with free biotin (upper panel) or treated with buffer only (lower panel), and visualized using Alexa Fluor 594-biocytin. b) Wild-type fd-tet and AP-tagged fd-tet-APpIII virions (10^{13}) were treated with BirA, followed by western blot visualized using SAV-HRP. c) BirA-treated fd-tet (upper panel) and fd-tet-APpIII (lower panel) phage virions (1.0×10^{10}) on SAV-SAM Au microspheres were detected using rabbit anti-fd antibody and anti-rabbit Alexa Fluor 610-R-PE antibody. In (a) and (c), left panels are bright-field light images; right panels are fluorescence images. d) Various amounts of biotinylated phage virions, prepared as in (b), were used for the titration of virus loading with the same reaction conditions as in (c).

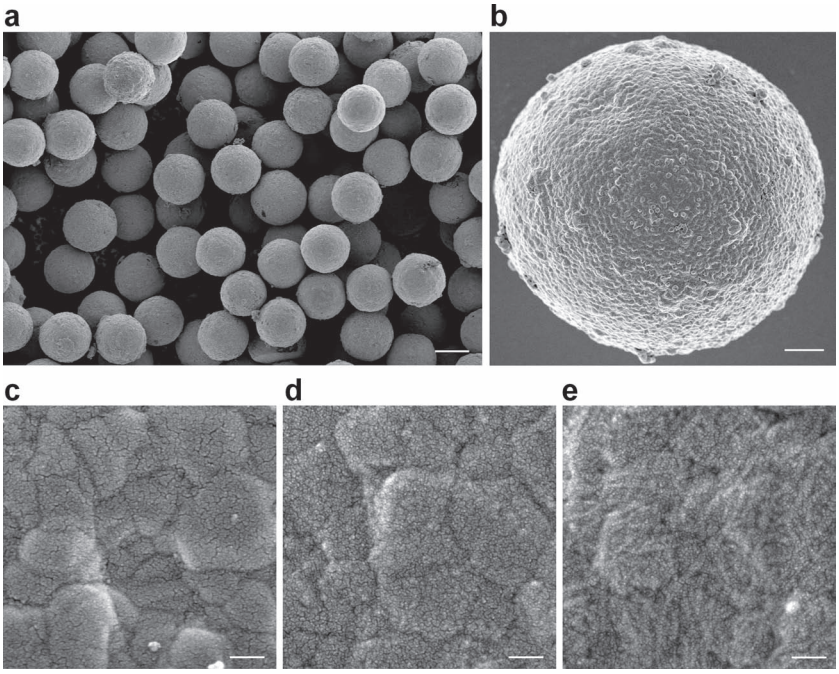

Figure 3. a) SEM image of magnetic Au microspheres (scale bar = 10 μm). b) Magnified image of Au microspheres reveals the morphology of Au layer (scale bar = 2 μm). Pt-sputtered surface morphology of the beads that had been modified with carboxyl-terminated hexa(ethylene glycol) undecane thiol SAM (c), then conjugated with SAV (d), and finally with pIII-biotinylated fd-tet phage virions (e). Scale bars for (c–e) are 100 nm.

was introduced in front of pIII, a tail of fd-tet bacteriophage that carries a tetracycline-resistance determinant.[15] Since the ε-amino group of Lys, a specific biotinylation site within the AP tag, is vulnerable to chemical modification by NHS for the subsequent Staudinger ligation, we tried in vivo biotinylation of phages by endogenous biotin ligase BirA that recognize AP in bacterial cells.[14] The degree of in vivo biotinylation, however, was minute, making us to purify BirA and biotinylate the virions in vitro.[16] When we incubated AP containing phage (fd-tet-APpIII) with BirA, clear bands (≈60 kD) appeared in western blot using SAV conjugated with horseradish peroxidase (SAV-HRP) (Figure 2b). We then briefly evaluated the loading of virions on SAV-Au microspheres and found saturated fluorescence signals using 1.0×10^{10} virions and 5 μg of SAV-Au microspheres (Figure 2c). Given that the apparent diameter of terminal N1-N2 domain of pIII is ≈6 nm and the tail part of the fd virus is composed of three to five copies of pIII,[17] one virion may be ensconced in an area of ≈8.5×10^{-17}–1.4×10^{-16} m^2. Since 5 μg of Au microspheres corresponds to ≈1000 beads, the total surface area of the beads is ≈7×10^{-7} m^2 on which ≈5–8 $\times 10^9$ of virions can be accommodated without gaps in theory. Indeed, when we titrated the loading of virions on the microspheres, the fluorescence intensity began to plateau from 1.0×10^{10} virions near the theoretical value (Figure 2d). Thus, we used 1.0×10^{10} virions to maximize antibody loading for subsequent immunoassays, while keeping the efficiency in phage preparation.

We next compared the surfaces of Au microspheres before and after the phage immobilization. **Figure 3**a,b are the FE-SEM images of bare Au microspheres that reveal Au granules layered on the surface of microspheres. After thiol SAM formation, Au surface maintained the overall roughness similar to the bare Au surface (Figure 3c). By contrast, SAV-modified surface exhibited tiny pimples, believed to be Pt-coated SAV, added on the Au granular blocks (Figure 3d and Figure S2, Supporting Information). Furthermore, in the case of virus-modified surface, we could clearly identify the virion fibers on the SAV layer with the increased thicknesses of 10–15 nm due to the sputtered Pt (Figure 3e and Figure S3, Supporting Information). The virion strands appeared to lie down because of the dry conditions and Pt sputtering required for the FE-SEM operation.

We then optimized antibody labeling with either amine-reactive NHS-PEG_{12}-azide or sulfo-NHS-phosphine. In our experimental conditions, antibody precipitated after incubation with sulfo-NHS-phosphine probably because of the increased hydrophobicity stems from the phenyl groups of phosphine. On the contrary, no antibody precipitate was found with NHS-PEG_{12}-azide, and no visible changes of SAV- and virus-beads were observed after labeling with sulfo-NHS-phosphine; SAV is already fixed on the beads, allowing no further aggregation, and phages are rich in surface charges that negate the effect of increased hydrophobicity. After ligation of the azide-modified primary antibody and the phosphine-modified beads, we stained the beads with fluorochrome-labeled secondary antibody and measured the fluorescence intensity of the beads. We found that the optimum concentration of phosphine was around 0.5 mM with 100 μM azide where, among others, the virus-tethered beads exhibited the highest fluorescence intensity (**Figure 4**a). The efficiency of antibody loading decreased at higher concentration of azide (1.0 mM) probably because of the limited access of secondary antibody to buried epitopes of the primary antibody. Lower amount of azide (20 μM) did not seem to push efficacious Staudinger ligation (Figure 4b). However, we cannot rule out the possibility that the lower the level of azide modification, the better the antibody activity.

To demonstrate the effect of long virus threads, after antibody loading we compared the biomimetic virus-beads with SAV-coated beads in terms of antibody activity against cardiac marker proteins, cardiac troponin I (cTnI) and myoglobin. We focused on the low range of cTnI and relatively higher range of myoglobin concentrations on the basis of clinical applications.[18] In immunoassays using cTnI- and myoglobin-spiked PBS, virus-decorated Au microspheres showed markedly enhanced signals compared to SAV-modified Au microspheres (**Figure 5**a,b). We could detect as low as 0.2 ng mL^{-1} of cTnI and myoglobin using virus-beads. The signals from SAV-beads lingered with the background until the concentration reached 2.0 ng mL^{-1} of cTnI and myoglobin. The effect of virions was more dramatic in the higher range of cTnI concentration with up to 9-fold increase in fluorescence signal at 10 ng mL^{-1}, while

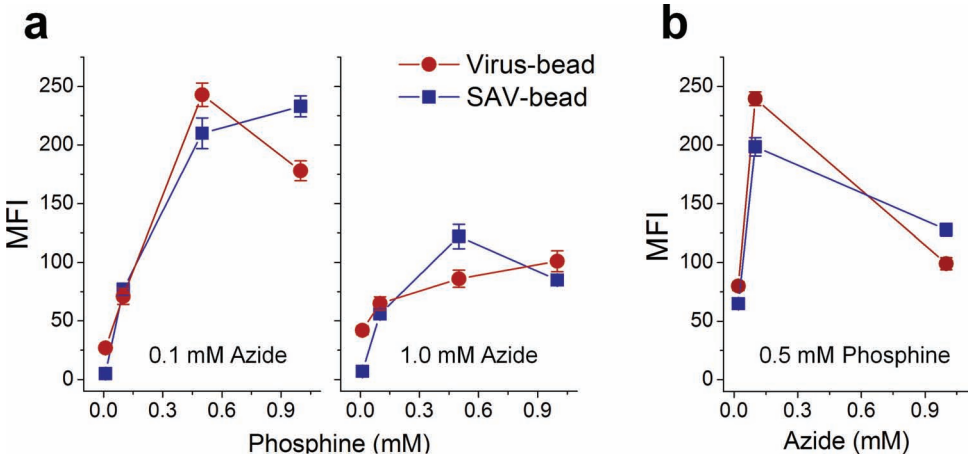

Figure 4. Optimization of Staudinger ligation using mouse antibody. a) Au microspheres, covered with SAV or phage virions, were treated with four different concentrations of sulfo-NHS-phosphine, while mouse antibody were incubated with 0.1 mM and 1.0 mM NHS-PEG_{12}-azide. b) SAV or phage-covered Au microspheres were incubated with fixed concentration of phosphine (0.5 mM), while the concentration of azide varied. Anti-mouse Alexa Fluor 594 antibody was used for the determination of mean fluorescence intensity (MFI).

the effect of virions on myoglobin showed two-fold increase within the concentration range tested. The difference in fold increase may originate from the intrinsic variances of antigens, such as size, structure, and binding constant to primary antibodies. Note that the difference in assay performance is greater than the one in the antibody loading between the SAV- and virus-beads (see Figure 4). Furthermore, the effect of viral fibers stands out when the amount of captured antigens, and thus the detection antibodies in sandwich assay, is limiting. Therefore, the enhanced sensitivity of the virus-beads may be ascribed to the greater amount of antibody and the long and flexible virus filaments that increase receptor-ligand interactions.

The preventive role of SAM-Au layer for non-specific adsorption was marked in immunoassays using serum samples that were spiked with cTnI. Interestingly, both virus- and SAV-beads detected as low as 20 pg mL^{-1} of cTnI (Figure 5c), while the SAV-beads exhibited partial improvement at higher concentration of cTnI (10 ng mL^{-1}) with two fold lower sensitivity than the

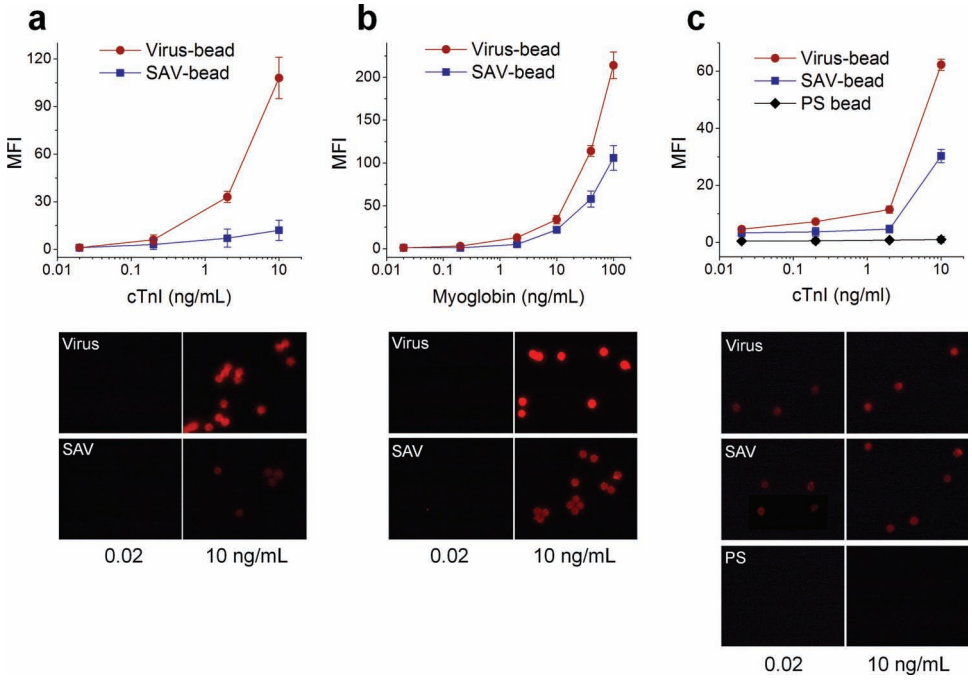

Figure 5. Sandwich immunoassay profiles (top) and representitive fluorescence images of each functionalized microspheres corresponding to the initial and final concentrations (bottom) tested for cardiac marker proteins. A range of cTnI in PBS (a), myoglobin in PBS (b), and cTnI in serum (c) were detected using virus- and SAV-Au microspheres (a and b), as well as polymer microspheres (c).

virus-beads. Importantly, we observed concentration-dependent increase of fluorescence signals at lower range of cTnI only in the case of virus-beads. By contrast, typical carboxylated polystyrene (PS) beads, on which antibodies were conjugated with EDC-NHS chemistry, failed to produce any signals throughout the range tested in serum, although the beads were able to detect cTnI in PBS (Figure S4, Supporting Information). The reason why the sensitivity for cTnI in serum should increase remains obscure, although the results suggest that the dense antibodies on phage tentacles and the SAM-Au protection layer synergistically enhance the sensitivity for the lower range of marker proteins.

3. Conclusions

In cellular systems, threadlike protruding structures have been evolved to sustain efficacious cellular functions, such as cellular uptake of small- and large molecules, cellular adhesions to biological and non-biological matrices, cell-cell interactions, and ligand-receptor interactions. Inspired by the cellular morphology and by the additive effect of long tethers on receptor-ligand interactions, we decorated SAM-protected Au microspheres with filamentous virions that mimic microvilli-like biological architectures. The SAM-protected virus-Au microspheres showed extremely low non-specific bindings, enhanced capacity of antibody loading, and superior performance in immunoassays when compared with polymer beads and non-viral SAV-Au beads. The Au-protected and virus-tethered microbeads that resemble biological architectures will open up new possibilities for developing biocompatible and bio-inspired biosensors for the improved immunoassay.

4. Experimental Section

Materials: Sulfo-*N*-hydroxysulfosuccinimide (Sulfo-NHS), sulfo-NHS-phosphine, NHS-PEG_{12}-azide, and 1-ethyl-3-[3-dimethylaminopropyl] carbodiimide hydrochloride (EDC) were purchased from Thermo Scientific (Rockford, IL). Carboxyl-terminated hexa(ethylene glycol) undecane thiol (CMT002) was obtained from Nanoscience Instruments (Phoenix, AZ). Carbenicillin (Carb) and isopropyl β-D-1-thiogalactopyranoside (IPTG) were from Gold Biotechnology (St. Louis, MO). Streptavidin (SAV), bovine serum albumin (BSA), tetracycline (Tet), Tween-20, adenosine 5′-triphosphate (ATP), and cardiac troponin I (cTnI) were purchased from Sigma-Aldrich (St. Louis, MO). Plasmid pET21a-BirA was obtained from Addgene (Cambridge, MA). Magnetic gold microspheres (M-NG0501, Nomadien.com) were generated using proprietary methods including electroless plating of auric acids on proprietary magnetic poly(methyl methacrylate) (PMMA) beads (Nomadien.com) that were 15 μm in diameter. Nominal 10 μm diameter carboxylated polystyrene (PS) beads were from Polysciences (Warrington, PA). Phage vector, fd-tet with *Sfi*I and *Not*I cloning site in front of pIII, was kindly provided by Drs. Philipp Holliger and Chang-Hoon Nam. Rabbit polyclonal anti-fd (ab6188) and anti-cTnI (ab47003) antibodies were purchased from Abcam (Cambridge, MA). Mouse monoclonal anti-cTnI antibody [19C7] was from GeneTex (Irvine, CA). Chicken Alexa Fluor 594 anti-mouse antibody (A21201), goat Alexa Fluor 610-R-Phycoerythrin (PE) anti-rabbit antibody, Alexa Fluor 594 biocytin, streptavidin conjugated with horseradish peroxidase (SAV-HRP), biotin, and bacterial cell lines for protein expression and phage amplification were obtained from Invitrogen (Carlsbad, CA). Myoglobin, rabbit polyclonal anti-myoglobin antibody (70-MR13), and mouse monoclonal anti-myoglobin antibody (10-M50A) were from Fitzgerald (North Acton, MA).

Fluorescence Microscopy: Au microspheres (≈100) in phosphate-buffered saline (PBS, 5 μL) were spotted on a glass slide. The fluorescence was monitored using Olympus IX71 (Olympus, Japan) equipped with DXM-1200C CCD camera (Nikon, Japan). At least ten microspheres were chosen for the determination of mean fluorescence intensity (MFI) using NIS-Elements software version 2.30 (Nikon, Japan).

Field-Emission Scanning Electron Microscopy (FE-SEM): The surface morphology of Au microspheres on a carbon tape was monitored using JSM 5410LV (JEOL, Japan) with 2 kV of acceleration voltage at the National Instrumentation Center for Environmental Management (NICEM), Seoul National University. To monitor the surface morphology of Au microspheres modified with thiol SAM, SAV, and phage virions, Pt was sputtered using BAL-TEC SCD 005 sputter coater at 15 mA for 100 s.

Production of BirA: His-tagged BirA was prepared according to the provider's protocol[14] with conditional modifications. Briefly, the pET21a-BirA plasmid was transformed into *E. coli* BL21(DE3)pLysS, plated on lysogeny broth (LB)-agar with Carb (100 μg mL^{-1}). A single colony was inoculated into LB-Carb media and was grown until the cell density reached mid-log phase when IPTG (1.0 mM) was added for induction. After overnight incubation at 37 °C, the cells were harvested, broken by sonication, and centrifuged. The supernatant was loaded onto Ni-NTA column to purify His-tagged BirA. Typically, a small-scale pilot test was performed using seven individual colonies when the best-expressing colony was used for the large-scale enzyme preparation.

Production of Phages Carrying Biotinylation Motif: The two primers, AP-F (5′-CGG CCA TGG CAG GTC TGA ACG ACA TCT TCG AGG CTC AGA AAA TCG AAT GGC ACG AAG GCT CCG GTG C-3′) and AP-R (5′-GGC CGC ACC GGA GCC TTC GTG CCA TTC GAT TTT CTG AGC CTC GAA GAT GTC GTT CAG ACC TGC CAT GGC CGG CT-3′), were annealed and ligated with fd-tet phage vector that had been digested with *Sfi*I and *Not*I. After the verification of the ligation by DNA sequencing, the phage vector was transformed into *E. coli* TG1 and grown in LB agar plate containing Tet (40 μg mL^{-1}) for 16 h at 37 °C. Next morning, a single colony was picked and inoculated into 3 mL of NZY liquid media with Tet (20 μg mL^{-1}) as a starter culture. For large-scale phage preparation, the starter culture was inoculated into NZY-Tet media (400 mL) and grown for 16 h at 37 °C with vigorous shaking. Phages were then purified by polyethylene glycol (PEG)/NaCl precipitation according to the standard protocols.[6]

Biotinylation of Phages: The purified phage virions (10^{13}) were incubated with BirA (30 nM), biotin (100 μM), and ATP (1 mM) in PBS-Mg (0.5 mL, pH 7.4 with 5 mM $MgCl_2$) for 2 h at 37 °C. The phages were then precipitated by PEG/NaCl two times and the residual PEG/NaCl molecules were removed by buffer exchange using Centricon (MWCO = 100 kDa). The level of biotinylation was evaluated by western blot using streptavidin-HRP.

Surface Modifications of Au Microspheres: Au microspheres (1 mg) was rotary incubated with carboxyl-terminated hexa(ethylene glycol) undecane thiol (1 mM) in 0.5 mL of ethanol for 16 h at 25 °C. To the SAM-modified Au microspheres (5 μg) was added EDC (2 mM) and NHS (5 mM) in 0.5 mL of MES buffer, pH 5.0 for 30 min at 25 °C. The beads were then washed with PBS (1 mL, pH 7.4) three times, followed by the addition of SAV (0.5 mg) in PBS (50 μL). The SAV-modified microspheres were treated with PBS-BT (PBS with 1% BSA, 0.1% Tween-20, pH 7.4) for 30 min and the SAV loading was verified using biocytin-Alexa Fluor 594.

Optimization of Phage Loading onto Au Microspheres: A range of biotinylated phage virions were rotary incubated with SAV-modified Au microspheres (5 μg) in PBS-BT (50 μL) for 16 h at 25 °C. As a negative control, wild-type fd-tet virions were used. After washing three times with PBS, the beads were treated with anti-fd rabbit IgG (37 ng) in PBS (50 μL) for 1 h at 25 °C. After washing, the loading of phage virions were visualized by incubating with anti-rabbit Alexa Fluor 610-R-PE antibody (100 ng) in PBS (50 μL) for 1 h at 25 °C, followed by the monitoring with a fluorescence microscope.

Optimization of Staudinger Ligation: SAV-modifed beads (5 μg) were incubated with varying amount of sulfo-NHS-phosphine in PBS (0.5 mL) for 1 h at 25 °C, which were used as a positive control. To build

virus-immobilized beads, the SAV-modified beads were further incubated with 1.0×10^{10} of biotinylated phages in PBS-BT (50 µL) for 16 h at 25 °C, washed three times with PBS-BT and three times with PBS, followed by an incubation with a range of Sulfo-NHS-Phosphine in PBS (0.5 mL) for 1 h at 25 °C. For the Staudinger ligation, primary antibody from mouse (100 µg) was incubated with NHS-$PEG_{12...}$-azide (0.1 and 1.0 mM) in of PBS (0.1 mL) for 1 h at 25 °C, followed by overnight dialysis against PBS. The phosphine-treated SAV- and virus-Au microspheres (5 µg) were ligated with the azide-modified mouse antibody (0.5 µg) in PBS for 4 h at 37 °C. The resulting beads were then washed three times with PBS-BT, followed by the incubation with anti-mouse Alexa Fluor 594 antibody for the fluorescence microscopic analysis. As a negative control, anti-mouse Alexa Fluor 594 antibody was directly treated with SAV- and virus-beads without azide-modified antibody and the background signals, if any, were subtracted.

Cardiac Marker Assays: Initially, the SAV- and virus-Au microspheres (5 µg) were treated with sulfo-NHS-phosphine (0.5 mM) in PBS (0.5 mL) for 1 h at 25 °C, followed by the ligation with rabbit polyclonal anti-cTnI capture antibodies (0.5 µg) that had been incubated with NHS-PEG_{12}-azide (100 µM) in PBS (50 µL) for 4 h at 37 °C. The resulting beads were then washed three times with PBS-BT and were mixed with cTnI (0.02, 0.2, 2, and 10 ng mL^{-1}) or myoglobin (0.02, 0.2, 2, 10, 40, and 100 ng mL^{-1}) in PBS (0.5 mL) for 1 h at 25 °C. For the detection of cTnI in human serum, PBS was replaced with cTnI-spiked human serum (0.02, 0.2, 2, and 10 ng mL^{-1} in 0.5 mL). The beads were then washed, incubated with mouse monoclonal anti-cTnI detection antibody [19C7] in PBS (500 ng, 50 µL) for 1 h at 25 °C, and visualized with anti-mouse Alexa Fluor 594 antibody (500 ng). For the determination of background signals, the assay was performed using the same conditions without marker proteins.

Supporting Information

Supporting Information is available from the Wiley Online Library or from the author.

Acknowledgements

The authors thank Dr. Philipp Holliger at the MRC Laboratory of Molecular Biology (U.K.) and Dr. Chang-Hoon Nam at the KIST-Europe (Germany) for providing phage vectors and Ms. Eun Byul Kook and Ms. Hyun-Ae Ryu for their technical assistance. The research was supported in part by the National Research Foundation of Korea (NRF) grant funded by the Ministry of Education, Science and Technology (MEST) (No. 2012011289), the Public Welfare & Safety Research Program through the NRF funded by the MEST (No. 2010-0020780), and the Technology Innovation Program (10041596, Development of Core Technology for TFT Free Active Matrix Addressing Color Electronic Paper with Day and Night Usage) funded by the Ministry of Knowledge Economy (MKE, Korea).

Received: August 31, 2012
Published online: October 26, 2012

[1] C. B. Mao, A. H. Liu, B. R. Cao, *Angew. Chem. Int. Ed.* **2009**, *48*, 6790.
[2] a) L. M. Chen, A. J. Zurita, P. U. Ardelt, R. J. Giordano, W. Arap, R. Pasqualini, *Chem. Biol.* **2004**, *11*, 1081; b) R. Edgar, M. McKinstry, J. Hwang, A. B. Oppenheim, R. A. Fekete, G. Giulian, C. Merril, K. Nagashima, S. Adhya, *Proc. Natl. Acad. Sci. USA* **2006**, *103*, 4841; c) K. Li, Y. Chen, S. Q. Li, G. N. Huong, Z. W. Niu, S. J. You, C. M. Mello, X. B. Lu, Q. A. Wang, *Bioconjugate Chem.* **2010**, *21*, 1369; d) S. Horikawa, D. Bedi, S. Q. Li, W. Shen, S. C. Huang, I. H. Chen, Y. T. Chai, M. L. Auad, M. J. Bozack, J. M. Barbaree, V. A. Petrenko, B. A. Chin, *Biosens. Bioelectron.* **2011**, *26*, 2361; e) J. A. Arter, J. E. Diaz, K. C. Donavan, T. Yuan, R. M. Penner, G. A. Weiss, *Anal. Chem.* **2012**, *84*, 2776.
[3] a) G. R. Souza, D. R. Christianson, F. I. Staquicini, M. G. Ozawa, E. Y. Snyder, R. L. Sidman, J. H. Miller, W. Arap, R. Pasqualini, *Proc. Natl. Acad. Sci. USA* **2006**, *103*, 1215; b) L. M. C. Yang, P. Y. Tam, B. J. Murray, T. M. McIntire, C. M. Overstreet, G. A. Weiss, R. M. Penner, *Anal. Chem.* **2006**, *78*, 3265; c) L. M. C. Yang, J. E. Diaz, T. M. McIntire, G. A. Weiss, R. M. Penner, *Anal. Chem.* **2008**, *80*, 933; d) N. F. Steinmetz, E. Bock, R. P. Richter, J. P. Spatz, G. P. Lomonossoff, D. J. Evans, *Biomacromolecules* **2008**, *9*, 456; e) J. S. Park, M. K. Cho, E. J. Lee, K. Y. Ahn, K. E. Lee, J. H. Jung, Y. J. Cho, S. S. Han, Y. K. Kim, J. Lee, *Nat. Nanotechnol.* **2009**, *4*, 259; f) J. A. Arter, D. K. Taggart, T. M. McIntire, R. M. Penner, G. A. Weiss, *Nano Lett.* **2010**, *10*, 4858; g) J. H. Lee, J. N. Cha, *Anal. Chem.* **2011**, *83*, 3516; h) K. C. Donavan, J. A. Arter, R. Pilolli, N. Cioffi, G. A. Weiss, R. M. Penner, *Anal. Chem.* **2011**, *83*, 2420; i) J. H. Lee, D. W. Domaille, J. N. Cha, *ACS Nano* **2012**.
[4] R. Wilson, A. R. Cossins, D. G. Spiller, *Angew. Chem. Int. Ed.* **2006**, *45*, 6104.
[5] a) J. C. Love, L. A. Estroff, J. K. Kriebel, R. G. Nuzzo, G. M. Whitesides, *Chem. Rev.* **2005**, *105*, 1103; b) M. Schaeferling, S. Schiller, H. Paul, M. Kruschina, P. Pavlickova, M. Meerkamp, C. Giammasi, D. Kambhampati, *Electrophoresis* **2002**, *23*, 3097; c) C. J. Huang, Y. T. Li, S. Y. Jiang, *Anal. Chem.* **2012**, *84*, 3440.
[6] C. F. Barbas, *Phage display: a laboratory manual*, Cold Spring Harbor Laboratory Press, Cold Spring Harbor, NY **2001**.
[7] a) Y. S. Nam, T. Shin, H. Park, A. P. Magyar, K. Choi, G. Fantner, K. A. Nelson, A. M. Belcher, *J. Am. Chem. Soc.* **2010**, *132*, 1462; b) J. R. Newton, Y. B. Miao, S. L. Deutscher, T. P. Quinn, *J. Nucl. Med.* **2007**, *48*, 429; c) J. Muzard, M. Platt, G. U. Lee, *Small* **2012**, *8*, 2403.
[8] G. P. Smith, V. A. Petrenko, *Chem. Rev.* **1997**, *97*, 391.
[9] a) C. Jeppesen, J. Y. Wong, T. L. Kuhl, J. N. Israelachvili, N. Mullah, S. Zalipsky, C. M. Marques, *Science* **2001**, *293*, 465; b) B. E. Collins, J. C. Paulson, *Curr. Opin. Chem. Biol.* **2004**, *8*, 617; c) S. H. Wang, E. E. Dormidontova, *Soft Matter* **2011**, *7*, 4435; d) D. Reeves, K. Cheveralls, J. Kondev, *Phys. Rev. E* **2011**, *84*.
[10] M. F. Bear, B. W. Connors, M. A. Paradiso, *Neuroscience: exploring the brain*, Lippincott Williams & Wilkins, Philadelphia, PA **2007**.
[11] G. Greicius, L. Westerberg, E. J. Davey, E. Buentke, A. Scheynius, J. Thyberg, E. Severinson, *Int. Immunol.* **2004**, *16*, 353.
[12] a) H. Connell, W. Agace, P. Klemm, M. Schembri, S. Marild, C. Svanborg, *Proc. Natl. Acad. Sci. USA* **1996**, *93*, 9827; b) J. Lederberg, E. L. Tatum, *Nature* **1946**, *158*, 558.
[13] E. Saxon, C. R. Bertozzi, *Science* **2000**, *287*, 2007.
[14] M. Howarth, A. Y. Ting, *Nat. Protoc.* **2008**, *3*, 534.
[15] A. N. Zacher, C. A. Stock, J. W. Golden, G. P. Smith, *Gene* **1980**, *9*, 127.
[16] M. D. Scholle, U. Kriplani, A. Pabon, K. Sishtla, M. J. Glucksman, B. K. Kay, *ChemBioChem* **2006**, *7*, 834.
[17] P. Holliger, L. Riechmann, R. L. Williams, *J. Mol. Biol.* **1999**, *288*, 649.
[18] R. H. Christenson, H. M. E. Azzazy, *Clin. Biochem.* **2009**, *42*, 150.
[19] W. Humphrey, A. Dalke, K. Schulten, *J. Mol. Graphics Modell.* **1996**, *14*, 33.